ChemComm

Accepted Manuscript

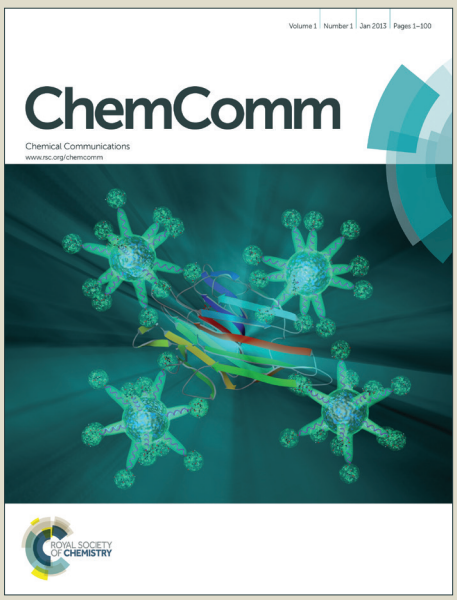

ROYAL SOCIETY OF CHEMISTRY

www.rsc.org/chemcomm

Journal Name

RSCPublishing

COMMUNICATION

Guanosine radical reactivity explored by pulse radiolysis coupled with transient electrochemistry.

Cite this: DOI: 10.1039/xoxxoooooox

A. Latus,[a,b] M. S. Alam,[a,b] M. Mostafavi,[c] J-L. Marignier*[c] and E. Maisonhaute*[a,b]

Received ooth January 2012,
Accepted ooth January 2012

DOI: 10.1039/xoxxoooooox

www.rsc.org/

We follow the reactivity of guanosine radical created by a radiolytic electron pulse both by spectroscopic and electrochemical methods. This original approach allows to demonstrate that there is a competition between oxidation and reduction of these intermediates, an important result to further analyse degradation or repair paths of DNA bases.

Oxidative stress agents' reactivity with DNA bases is still under high focus. These oxidants may be produced internally by biological reaction cascades or from external aggressions such as those induced by ionizing radiations.[1] In aqueous solutions, radiations cause breakdown of water that forms the so-called primary species as described in equation (1) of scheme 1. Among them hydroxyl radical $OH^{\bullet}$ is a very strong oxidant[2] that can either react directly with DNA bases or with other molecules of the cell to produce various oxidants that are also potentially aggressive for DNA or different systems such as proteins.[3-5] For long, it has been demonstrated that the guanine entity is the most sensitive DNA base towards oxidants.[1, 6] For example, Giese et al. located a first oxidative damage at a precise position of a DNA double strand, and demonstrated that it could migrate over distances up to more than 5 nm to end up onto a guanine entity.[7] In DNA, GG or GGG sequences are even more easily oxidized. Therefore, it is of great interest to decipher DNA reactivity, and more specifically the one of guanine derivatives, with one-electron oxidants.

For fundamental and analytical purposes, there have been also numerous studies onto DNA using electrochemical methodologies.[6] However, in water, mechanistic studies are extremely difficult because up to 4 electrons and 4 protons may be transferred.[8] Moreover, adsorption may render even more complex the electrochemical analysis.[9] As a consequence, cyclic voltammograms are usually poorly resolved. To this respect, redox catalysis allows to work with low concentrations, minimizing adsorption or solubility problems, but then access to the chemical mechanism is only indirect.[10, 11] Another alternative is to work in organic solvent. For example, in order to decipher the interaction mechanism of guanine with cytosine, Saveant et al. shifted from water to chloroform.[12] There would be, however, a considerable interest to introduce an electrochemical methodology for working in physiological conditions.

An alternative methodology for inducing redox processes stems from pulse radiolysis. Here, by using specific adjuvants a controlled one electron oxidation can be triggered in water. This strategy was successfully employed by O'Neill first to identify the spectrum of desoxyriboseguanosine radical at neutral pH.[13] The mechanism of several guanosine (**G**) derivatives was later completed by Steenken et al.[12, 13] It was demonstrated that at neutral pH deprotonation of the first radical $\mathbf{G}^{\bullet+}$ occurs very quickly, leading to the more stable neutral radical $\mathbf{G(-H)}^{\bullet}$.[14, 15] Furthermore, competitive kinetics with redox mediator was used first by Simic et al.,[16] then by Steenken[17] to evaluate the apparent redox potential of $\mathbf{G(-H)}^{\bullet}/\mathbf{G}$. A value of 1.29 V *vs* ESH at pH = 7 was found. In pulse radiolysis, reactions are blocked at a single electron transfer level because an excess of **G** is present, compared to the concentration of oxidant produced following the radiolytic pulse. Another advantage is that micro-molar radical concentrations are produced, hence much closer to physiological conditions. While traditional detection in pulse radiolysis experiments is performed spectroscopically, we thought that replacing the redox mediator by an electrode to monitor a direct collection of electrons would represent an additional complementary methodology. Bearing in mind advantages and drawbacks of both pulse radiolysis and electrochemistry, we then reactivated recently a transient electrochemical detection of the radicals initiated by an electron pulse. This interesting strategy was originally pioneered by Henglein et al. in the seventies, but then abandoned.[18] With present modern instrumentation in both pulse radiolysis and transient electrochemistry, we below explore the one-electron oxidation of guanosine and guanosine monophosphate by the well-behaved $Br_2^{\bullet-}$ radical. Our results highlight the potentiality of this approach for analysing with *in vitro* experiments the complex reactivity of biological intermediates.

In our setup, a 7-8 MeV electron pulse is sent onto an electrode immersed in the solution to be studied and polarized at a constant

potential.[19] The typical duration of the pulse is around 10 ps. Detection is performed both spectroscopically with a nanosecond resolution, and amperometrically with a submillisecond resolution. The experimental set-up was similar to what we previously described (see ESI for more details).[20] In the following, **G** represents either guanosine or guanosine monophosphate. As demonstrated below, the mechanism is identical for both systems, so that in the following figures we alternatively present data for guanosine or guanosine monophosphate. The complementary set of data is presented in ESI. An aqueous solution containing 1 mM **G**, 0.1 M KBr and 0.1 M phosphate buffer to ensure pH = 7.1 was first irradiated. To realize oxidative conditions, the solvated electrons and hydrogen atoms were quenched by bubbling N_2O in the solution. In those conditions, it is well established that the reaction sequence follows scheme 1:[13, 14, 21]

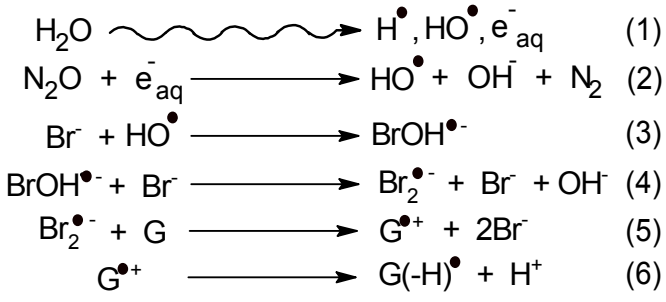

Scheme 1. Mechanism of guanosine oxidation by $Br_2^{\bullet-}$.

In the solution, $OH^{\bullet}$ reacts with Br^- to produce $BrOH^{\bullet-}$ and then $Br_2^{\bullet-}$.[21] Then, $Br_2^{\bullet-}$ oxidizes guanosine. The disproportionation of $Br_2^{\bullet-}$ could be neglected towards the electron transfer to guanine which is in excess.

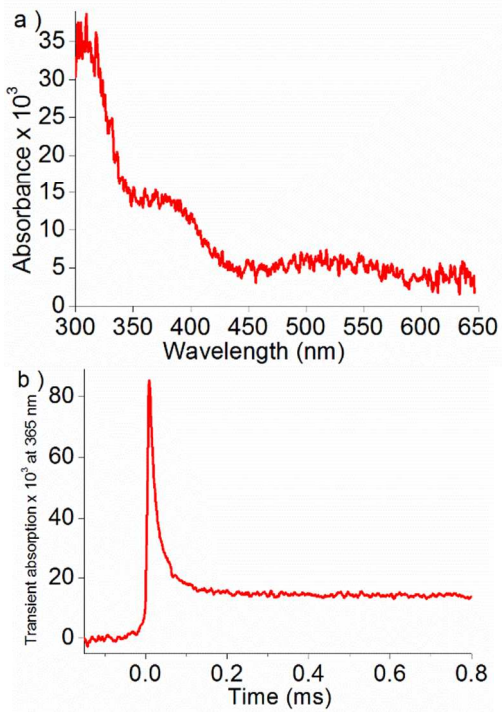

Figure 1. Transient spectroscopy of a 1 mM guanosine monophosphate solution upon oxidation by $Br_2^{\bullet-}$. a) Transient spectrum observed 250 µs after the pulse. b) Transient absorption at 365 nm.

This reaction was first followed by transient absorption measurements. Figure 1 represents the transient spectrum obtained 250 µs after the pulse and the transient absorption followed at 365 nm for a 1 mM **G** solution. These results are perfectly in line with literature, indicating production of a uniform concentration of **G(-H)**$^{\bullet}$ after 200 µs.[13-15, 22] Indeed, in figure 1b, the initial decrease corresponds simultaneously to disappearance of $Br_2^{\bullet-}$ and appearance of **G(-H)**$^{\bullet}$. With a dose of 38 Gy/pulse, a 28±4 µM concentration of **G(-H)**$^{\bullet}$ was produced. This latter radical decays over a longer time scale and we measured a second order rate of $k_{SO} = 1.2 \pm 0.3 \times 10^7$ $M^{-1}s^{-1}$ for guanosine monophosphate and $k_{SO} = 3.4 \pm 0.5 \times 10^7$ $M^{-1}s^{-1}$ for guanosine.

The mechanism being confirmed, we shifted to electrochemical detection with a gold electrode having an area of 6.6×10^{-3} cm^2. Here, the electrode potential was maintained in a window for which the baseline current was negligible. The electron pulse induced production of **G(-H)**$^{\bullet}$ as described above, which resulted in observation of current transients. For each potential, around 10 transients were acquired and averaged. Figure 2 presents the curves obtained after subtraction of a background transient signal. Since subtraction of this parasitic signal is accurate only after 300-500 µs, electrochemical data are relevant only after 500µs. Hence, production of **G(-H)**$^{\bullet}$ being extremely fast compared to the electrochemical timescale, we could reasonably consider that at t = 0 the solution contained a **G(-H)**$^{\bullet}$ concentration of 28 µM. Below 400 mV *vs* AgCl/Ag, the current traces were superimposable, indicating that only reduction occurred at a diffusion limited rate. The situation was however different from a standard chronoamperometric decay because dimerization of **G(-H)**$^{\bullet}$ in solution occurred in completion with reaction at the electrode surface. This interplay was taken into account by numerical simulations of this diffusion controlled reduction. This way, we could determine a bimolecular decay for **G(-H)**$^{\bullet}$ of $k_{SO} = 1.1 \pm 0.3 \times 10^7$ $M^{-1}s^{-1}$ for guanosine monophosphate and $3 \pm 1 \times 10^7$ $M^{-1}s^{-1}$ for guanosine, in complete agreement with spectroscopic measurements.

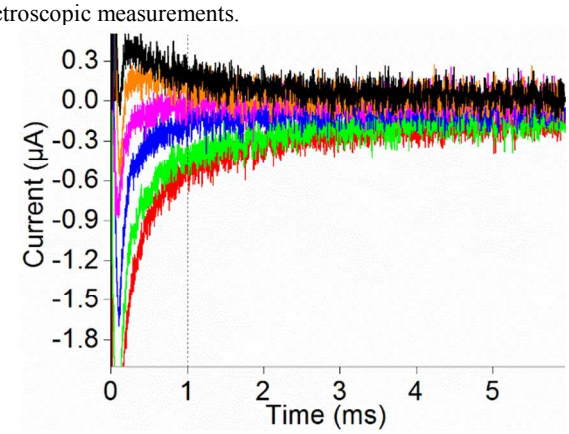

Figure 2. Oxidation of guanosine by $Br_2^{\bullet-}$. Transient electrochemical currents recorded at different potentials *vs* AgCl/Ag : -97 mV (red), 501 mV (green), 601 mV (blue), 618 mV (magenta), 651 mV (orange), 661 mV (black). Solution composition: 1 mM guanosine, 0.1 M KBr, 0.1 M phosphate buffer under N_2O saturation. Dose: 38 Gy/pulse (28 µM initial concentration in **G(-H)**$^{\bullet}$). pH = 7.1.

Once k_{SO} was determined, we focused on the current evolution in the whole potential range. A first evidence is a continuous shift from reduction to oxidation currents, the transition occurring near 0.63 V *vs* AgCl/Ag. This observation is in line with the so-called redox ambivalence observed by O'Neill and Steenken, *i.e.* the ability of this radical to be either oxidized or reduced.[13, 23] Such potential inversion is also frequent in electrochemical studies.[10, 24] We could not explore

higher potentials since direct oxidation of guanosine and gold oxide formation at the electrode interfered. To complete the description, similar experiments but with either a lower dose (10 Gy corresponding to a starting concentration of **G(-H)**$^{\bullet}$ of 7.3 µM) or for a different initial **G** concentration were also performed. Identical behaviors with a transition at the same potential were observed. These complementary results are displayed in ESI together with their analysis. These additional observations confirmed that no electron transfer equilibrium is attained at the electrode surface, as expected when working at electrode potentials far from the apparent standard potentials of the redox systems under investigation (see below). Since identical behavior is observed for both **G** derivatives having different solubility in water, any contribution from adsorption in the observed signal could be eliminated.

For further interpretation, the current value 1 ms after the pulse was recorded at each potential to trace reconstructed polarograms, as presented in figure 3a. Deviating from standard electrochemical systems, here the current *I* resulted from the difference between the one electron oxidation and reduction currents of **G(-H)**$^{\bullet}$ according to:[25]

$$\frac{I}{FA} = k_{\mathrm{ox}}[\mathrm{G}(-\mathrm{H})^{\bullet}]_{x=0} - k_{red}[\mathrm{G}(-\mathrm{H})^{\bullet}]_{x=0} \quad (1)$$

where k_{ox} and k_{red} are respectively the potential-dependent rates for oxidation and reduction of **G(-H)**$^{\bullet}$. *F*, *A* and *x* are the Faraday constant electrode area and distance from the electrode. A reduction plateau was obtained at low potentials, indicating predominance of reduction below 400 mV. Since electron transfer occurred far from the standard potentials, Marcus formulation should be preferred over Butler-Volmer's one in order to express k_{ox} and k_{red}.[10] For electrochemistry, we adapted a practical formulation taking into account the electrode density of states that was previously proposed by Chidsey so that:[26]

$$\frac{k_{\mathrm{ox}}}{k^0{}_{\mathrm{ox}}} = \frac{\mathrm{f}(E\text{-}E^{0'}{}_{\mathrm{ox}})}{\mathrm{f}(0)} \quad (2)$$

with

$$\mathrm{f}(E - E^{0\prime}{}_{\mathrm{ox}}) = \int_{-\infty}^{+\infty} \frac{exp((x-\frac{\lambda_{\mathrm{ox}}-E+E^{0\prime}{}_{\mathrm{ox}}}{k_B T})^2 \times \frac{k_{\mathrm{B}}T}{4\lambda_{\mathrm{ox}}})}{1+exp(x)} dx \quad (3)$$

and $\frac{k_{\mathrm{red}}}{k^0{}_{\mathrm{red}}} = \frac{\mathrm{g}(E\text{-}E^{0'}{}_{\mathrm{red}})}{\mathrm{g}(0)}$ (4)

with

$$\mathrm{g}(E - E^{0\prime}{}_{\mathrm{red}}) = \int_{-\infty}^{+\infty} \frac{exp((x-\frac{\lambda_{\mathrm{red}}+E-E^{0\prime}{}_{\mathrm{red}}}{k_B T})^2 \times \frac{k_{\mathrm{B}}T}{4\lambda_{\mathrm{red}}})}{1+exp(x)} dx \quad (5)$$

where $E^{0\prime}{}_{ox}$ and $E^{0\prime}{}_{red}$ are the apparent standard potentials at pH = 7.1, $k^0{}_{ox}$ and $k^0{}_{red}$ being the standard rate constant for oxidation and reduction processes, obtained for $E = E^{0\prime}{}_{ox}$ and $E = E^{0\prime}{}_{red}$ respectively. $k^0{}_{ox}$ and $k^0{}_{red}$ are strongly influenced by λ_{ox} and λ_{red}, the reorganization energies for both reactions. The main effect of using Marcus theory over Butler-Volmer's one is to damp the exponential variation of k_{ox} and k_{red} with the potential, and, consequently the slope of the polarogram displayed in figure 3a. In literature, only $E^{0\prime}{}_{red}$ = 1.29 ± 0.03 V *vs* ESH (1.09 V *vs* AgCl/Ag), proposed by Steenken, is available. To fit our data, we followed Saveant[12] and imposed $k^0{}_{ox} = k^0{}_{red}$ = 1 cms^{-1}.[12] Variations around this value did not affect the quality of the fit as expected from the full analysis depicted in ESI. The best agreement between experimental data and theory was obtained for the perfect symmetrical case where $E^{0\prime}{}_{ox}$ = 0.17 V *vs* AgCl/Ag, $\lambda_{ox} = \lambda_{red}$ = 0.9 eV. Such value of reorganization energy is completely in the range of what can be expected for this molecule.[6, 27] Also, it indicates that for the reduction process involving one electron and one proton, there is no additional contribution to the activation barrier due to the proton transfer. This is in line with a stepwise electron transfer followed by protonation, as already demonstrated in pulse radiolysis or electrochemistry for the oxidation process.[12, 14] Another important information is that indeed oxidation of **G(-H)**$^{\bullet}$ is very favorable, so that after the first electron transfer, even mild oxidants are capable of attacking **G(-H)**$^{\bullet}$ to yield **G(-H)**$^{+}$, and probably 8-oxoguanosine after H_2O addition and proton elimination.[3, 4] Yet, reparation by reduction with an anti-oxidant is also favored, underlining an extreme sensitivity of the reaction path on the cellular composition.[3, 4, 23]

Returning to the second order decay occurring in solution, a value much below 10^9-10^{10} M^{-1}s^{-1} for k_{SO} points to an activation and not diffusion limited reaction. A dimerization is postulated in the literature,[9, 12, 28] but the large potential inversion also stresses that disproportionation could be considered. Discriminating between these two possibilities was however beyond the scope of the present study.

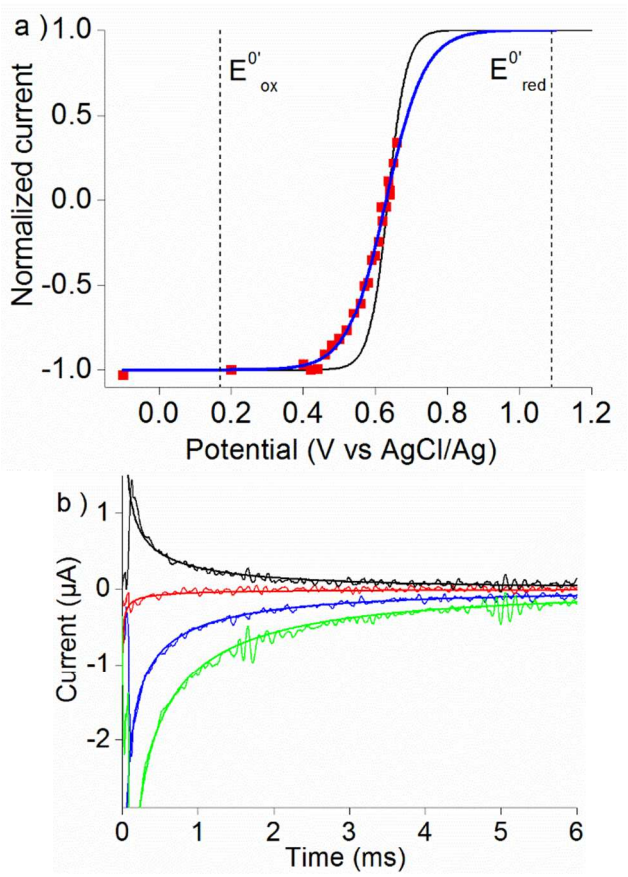

Figure 3. a) Reconstructed normalized polarogram obtained from figure 2 (guanosine) by measuring the current 1 ms after the pulse for each potential. Red dots: experimental data. Black line: simulation using Butler-Volmer formulation with $E^{0\prime}{}_{red}$ = 1.09 V, $E^{0\prime}{}_{ox}$ = 0.17 V, $k^0{}_{ox} = k^0{}_{red}$ = 1 cms^{-1} and α = 0.5. Blue line: simulation using Marcus theory with $E^0{}_1$ = 1.09 V, $E^0{}_2$ = 0.17 V, $k^0{}_{ox} = k^0{}_{red}$ = 1 cms^{-1} and $\lambda_{ox} = \lambda_{red}$ = 0.9 eV. b) Experimental (thin lines) and simulations (thick lines) of the current traces with the same parameters at 103 mV (green), 582 mV (blue), 621 mV (red) and 651 mV (black) *vs* AgCl/Ag for guanosine monophosphate. The raw data were resampled and filtered to attenuate the noise.

We then further simulated the temporal dependence of each current trace using the Digielch® software. As depicted in figure 3b, and figures S4 and S5, the agreement between experiment and theory is excellent. We furthermore noted that near $(E^{0'}_{ox} + E^{0'}_{red})/2$, simulation is extremely sensitive to the standard potentials, providing a precision of 10 mV on $E^{0'}_{ox}$. In the present study the precision is however limited to 30 mV since we relied on $E^{0'}_{red}$ = 1.09 ± 0.03V *vs* AgCl/Ag provided by Steenken. This complex mechanism is then fully deciphered thanks to a combined analysis of spectroscopic and electrochemical acquisitions.

Conclusions

The example of guanosine oxidation highlights the complementarity of the well-established spectroscopic detection of intermediates created by pulse radiolysis and the unusual electrochemical monitoring. Spectroscopy was a necessary control to confirm that the system reacted in agreement with literature. This technique is also necessary in evaluation of the dose, hence of the starting concentration of radicals. It furthermore provides access to very short timescales, allowing to follow fast kinetics. Moreover, the spectroscopic redox titration technique is useful to estimate the standard potentials but unfortunately not always successful. In contrast, the electrochemical methodology should be improved to reach shorter timescales but present the advantage of directly monitoring the electron fluxes. The modification of the driving force of electrochemical reactions is furthermore precisely tuned with the electrode potential. In the present case, the redox ambivalence was evidenced in a rather straightforward way and could be quantitatively analysed. The great interest of this methodology is the possibility to perform transient electrochemistry onto low (micro-molar) concentrations in a physiological environment. This minimizes drawbacks due to adsorption of products on the electrode surface due to their low solubility that often prevent their in depth electrochemical study to be performed in water. Future work may concern more complex systems such as the oxidation of small DNA oligomers[29, 30] and the effects of other oxidants.

This work was supported by ANR (project Radiolyse et Analyse Dynamique par Electrochimie, JCJC 0810). We thank Pr. Manfred Rudolph for helpful discussions about Marcus theory implementation into Digielch®.

Notes and references

[a] Sorbonne Universités, UPMC Univ Paris 06, UMR 8235, Laboratoire Interfaces et Systèmes Electrochimiques, F-75005 Paris, France. e-mail: emmanuel.maisonhaute@upmc.fr

[b] Sorbonne Universités, CNRS, UMR 8235, Laboratoire Interfaces et Systèmes Electrochimiques, F-75005 Paris, France.

[c] Laboratoire de Chimie Physique, CNRS UMR 8000, Université Paris-Sud, Bat 350, 91405 Orsay Cedex, France. e-mail: jean-louis.marignier@u-psud.fr.

Electronic Supplementary Information (ESI) available: details about the experimental procedure, simulation methodology, complementary spectroscopic and electrochemical data for guanosine or guanosine monophosphate. See DOI: 10.1039/b000000x/

1. D. Becker and M. D. Sevilla, in *Advances in Radiation Biology*, eds. J. T. Lett and W. K. Sinclair, San Diego, 1993, pp. 121-180.
2. E. Sutter, K. Jungjohann, S. Bliznakov, A. Courty, E. Maisonhaute, S. Tenney and P. Sutter, *Nat. Commun.*, 2014, 5, 4946.
3. J. Cadet, T. Douki and J. L. Ravanat, *Nat. Chem. Biol.*, 2006, 2, 348-349.
4. J. Cadet, T. Douki and J. L. Ravanat, *Accounts Chem. Res.*, 2008, 41, 1075-1083.
5. A. Et Taouil, E. Brun, P. Duchambon, Y. Blouquit, M. Gilles, E. Maisonhaute and C. Sicard-Roselli, *Phys. Chem. Chem. Phys.*, 2014, 16, 24493-24498.
6. F. Boussicault and M. Robert, *Chem. Rev.*, 2008, 108, 2622-2645.
7. B. Giese, *Annu. Rev. Biochem.*, 2002, 71, 51-70.
8. Q. Li, C. Batchelor-McAuley and R. G. Compton, *J. Phys. Chem. B*, 2010, 114, 7423-7428.
9. E. E. Ferapontova, *Electrochim. Acta*, 2004, 49, 1751-1759.
10. J.-M. Saveant, *Elements of Molecular and Biomolecular Electrochemistry*, John Wiley and Son, Hoboken, New Jersey, first edn., 2006.
11. H. Xie, D. W. Yang, A. Heller and Z. Q. Gao, *Biophys. J.*, 2007, 92, L70-L72.
12. C. Costentin, V. Hajj, M. Robert, J. M. Saveant and C. Tard, *J. Am. Chem. Soc.*, 2010, 132, 10142-10147.
13. P. O'Neill and P. W. Chapman, *Int. J. Radiat. Biol.*, 1985, 47, 71-80.
14. L. P. Candeias and S. Steenken, *J. Am. Chem. Soc.*, 1989, 111, 1094-1099.
15. C. Chatgilialoglu, C. Caminal, A. Altieri, G. C. Vougioukalakis, Q. G. Mulazzani, T. Gimisis and M. Guerra, *J. Am. Chem. Soc.*, 2006, 128, 13796-13805.
16. S. V. Jovanovic and M. G. Simic, *J. Phys. Chem.*, 1986, 90, 974-978.
17. S. Steenken and S. V. Jovanovic, *J. Am. Chem. Soc.*, 1997, 119, 617-618.
18. A. Henglein, in *Electroanalytical Chemistry - A Series of Advances*, ed. A. J. Bard, Marcel Dekker, New York, 1976, vol. 9, pp. 163-245.
19. J. L. Marignier, V. de Waele, H. Monard, F. Gobert, J. P. Larbre, A. Demarque, M. Mostafavi and J. Belloni, *Radiat. Phys. Chem.*, 2006, 75, 1024-1033.
20. M. S. Alam, E. Maisonhaute, D. Rose, A. Demarque, J. P. Larbre, J. L. Marignier and M. Mostafavi, *Electrochem. Commun.*, 2013, 35, 149-151.
21. M. Mirdamadi-Esfahani, I. Lampre, J. L. Marignier, V. de Waele and M. Mostafavi, *Radiat. Phys. Chem.*, 2009, 78, 106-111.
22. C. Chatgilialoglu, C. Caminal, M. Guerra and Q. G. Mulazzani, *Angew. Chem.-Int. Edit.*, 2005, 44, 6030-6032.
23. L. P. Candeias and S. Steenken, 2000, 6, 475-484.
24. C. Amatore, E. Maisonhaute, B. Schollhorn and J. Wadhawan, *Chemphyschem*, 2007, 8, 1321-1329.
25. K. M. Bansal and A. Henglein, *J. Phys. Chem.*, 1974, 78, 160-164.
26. C. E. D. Chidsey, *Science*, 1991, 251, 919-922.
27. K. Siriwong, A. A. Voityuk, M. D. Newton and N. Rosch, *J. Phys. Chem. B*, 2003, 107, 2595-2601.
28. M. Faraggi, F. Broitman, J. B. Trent and M. H. Klapper, *J. Phys. Chem.*, 1996, 100, 14751-14761.
29. K. Kobayashi and S. Tagawa, *J. Am. Chem. Soc.*, 2003, 125, 10213-10218.
30. Y. Rokhlenko, N. E. Geacintov and V. Shafirovich, *J. Am. Chem. Soc.*, 2012, 134, 4955-4962.

